# NASA TECHNICAL NOTE

NASA TN D-4079

c. 1
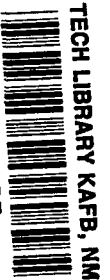
NASA TN D-4079

# HYPERSONIC AERODYNAMIC CHARACTERISTICS OF MINIMUM-WAVE-DRAG BODIES HAVING VARIATIONS IN CROSS-SECTIONAL SHAPE

*by Bernard Spencer, Jr.*

*Langley Research Center*
*Langley Station, Hampton, Va.*

NASA TN D-4079

HYPERSONIC AERODYNAMIC CHARACTERISTICS OF

MINIMUM-WAVE-DRAG BODIES HAVING VARIATIONS IN

CROSS-SECTIONAL SHAPE

By Bernard Spencer, Jr.

Langley Research Center
Langley Station, Hampton, Va.

NATIONAL AERONAUTICS AND SPACE ADMINISTRATION

# HYPERSONIC AERODYNAMIC CHARACTERISTICS OF
# MINIMUM-WAVE-DRAG BODIES HAVING VARIATIONS IN
# CROSS-SECTIONAL SHAPE

By Bernard Spencer, Jr.
Langley Research Center

## SUMMARY

An investigation has been made at hypersonic speeds of a series of bodies having variations in cross-sectional shape and camber. The longitudinal distribution of cross-sectional area for each body conformed to the theoretical shape required to minimize the zero-lift hypersonic pressure drag of circular or elliptic bodies under the geometric constraints of given length and volume. Each body tested had constant planform area, base area, and span; the only variables were cross-sectional shape, camber, and the resultant small wetted-area changes. Cross sections tested included semicircular, elliptic, triangular, trapezoidal, and rectangular shapes. Results indicated that changing cross-sectional shape with either positive or negative camber had essentially no effect on the minimum-drag characteristics of any configuration tested. For all cross sections investigated, the highest values of untrimmed maximum lift-drag ratio and lift at maximum untrimmed lift-drag ratio were obtained for the flat-bottom (positive camber) bodies having upright semicircular, trapezoidal, or triangular cross sections; that is, cross sections having maximum width at the bottom. Large out-of-trim (negative) pitching moments at maximum lift-drag ratio were noted, however, for the bodies with positive camber. The bodies with negative camber produced favorable (positive) pitching moments and a considerable reduction in the angle of attack for maximum lift-drag ratio as compared with that obtained for the bodies with positive camber. Reversing the camber from positive to negative for an upright trapezoidal configuration (that is, a configuration having its major horizontal cross-sectional area at the bottom) resulted in essentially the same values of maximum lift-drag ratio and lift at maximum lift-drag ratio as had been noted before the reversal of camber. This reversal to negative camber also provided favorable pitching-moment characteristics and resultantly large reductions in the angle of attack for maximum lift-drag ratio.

INTRODUCTION

Considerable theoretical and experimental effort is presently being devoted to the development of high aerodynamic performance for lifting bodies at hypersonic speeds. (For example, see refs. 1 to 5.) Because of the favorable relationship between volume and wetted area inherent in body shapes (as opposed to wings or wing-body combinations), considerable reduction in structural weight for vehicles designed either as manned spacecraft or hypersonic gliders should be realized. One approach toward improving hypersonic performance of lifting bodies has been to use bodies having longitudinal area distributions designed for minimizing zero-lift hypersonic pressure drag under certain prescribed geometric constraints and to modify the cross-sectional shape of such bodies from circular to elliptic. Results of studies utilizing this approach are summarized in reference 1. Increases in hypersonic lift-drag ratio of about 25 percent over that noted for an elliptic cone of equal length and volume resulted from use of the theoretical minimum-wave-drag body, although the lift coefficient at maximum lift-drag ratio was only about 60 percent of that noted for the cone. (See ref. 1.) Results of these studies have indicated the importance of minimizing the zero-lift pressure drag in improving the performance characteristics of lifting bodies.

Two problem areas noted from the studies of low-drag bodies in reference 1 are as follows: (1) The lift coefficient at maximum lift-drag ratio is low and (2) all results are out of trim — a fact which indicates that possible reductions in the maximum lift-drag ratios will result from control deflection, depending, of course, on resultant-moment reference location. In addition, cross-sectional shapes other than elliptic may be more desirable from structural-heating or personnel and payload-storage considerations. In consideration of cross-sectional shapes other than the circular or elliptic bodies studied in references 6 and 7, and to explain the insensitivity of the optimum longitudinal contour to alteration in cross section from a circle to an ellipse, as found in reference 7, Miele (ref. 8) has shown theoretically that there exists a similarity law for optimum bodies at hypersonic speeds which effectively notes that changes may be made in body cross-sectional shape, provided the optimum longitudinal contour for the basic circular axisymmetric (or reference) theoretical body is maintained. This longitudinal contour will then be optimum for the new cross section, provided the body is homothetic (i.e., each cross section is similar to the cross section at the base). Normalized area distributions for the basic minimum-drag circular bodies may be found in reference 1.

Since the use of the hypersonic minimum-drag body has proven useful in attaining improved hypersonic performance, the present investigation was initiated to examine the following items more fully: (1) The effects of body cross-sectional shape on the minimum-drag coefficient for these theoretical minimum-drag shapes, (2) the effects of cross-sectional shape on the maximum lift-drag ratio of these bodies as compared with

the basic elliptic body designed from minimum-hypersonic-wave-drag considerations, and (3) the effects of body camber for providing trimmed lift and lift-drag ratio. The longitudinal area distributions of the bodies of the present investigation were the zero-lift minimum-hypersonic-wave-drag contours determined for the prescribed geometric constraints of constant length and volume. (See refs. 1, 6, and 7.) The effective fineness ratio of the bodies was 5.0, with volume-length[3] ratio of 0.016. The planform area, base area, and longitudinal distribution of cross-sectional area were constant for each body, the only variables being cross-sectional shape, camber, and the resultant small wetted-area changes. Cross sections examined included upright and inverted semicircular, triangular, and trapezoidal shapes, as well as rectangular and elliptic shapes. The Mach number of the investigation was 10.03 corresponding to a Reynolds number (based on body length) of $1.40 \times 10^6$. The angle-of-attack range was from approximately $-5^o$ to $21^o$ at $0^o$ of sideslip.

## SYMBOLS

All longitudinal data are presented about the stability axes, and all coefficients have been normalized with respect to the projected planform area and length of each body (constant for all bodies). The longitudinal location of the moment reference point has been selected at 0.55 body length for each configuration. The vertical moment reference locations are shown for each body in figure 1.

$A_b$       cross-sectional area of body at base, feet$^2$ (meters$^2$)

$b$       height of body at base, feet (meters)

$C_{A,b}$       base axial-force coefficient, $\dfrac{p_b - p_\infty}{q_\infty}\left(\dfrac{A_b}{S}\right)$

$C_D$       drag coefficient, $\dfrac{\text{Drag}}{q_\infty S}$

$C_L$       lift coefficient, $\dfrac{\text{Lift}}{q_\infty S}$

$C_m$       pitching-moment coefficient, $\dfrac{\text{Pitching moment}}{q_\infty S \ell}$

$K$       ratio of minimum to maximum parallel horizontal surface spans for noncircular or nonelliptic family of bodies ($K = 1.0$ for rectangular bodies; $K = 0$ for triangular bodies; and $K = 1/2$ or $2/3$ for trapezoidal bodies), pounds/foot$^2$ (newtons/meter$^2$)

| $l$ | length of body, feet (meters) |
|---|---|

$l$      length of body, feet (meters)

L/D      lift-drag ratio

$M_\infty$      free-stream Mach number

$p_b$      static pressure at model base, pounds/foot$^2$ (newtons/meter$^2$)

$p_\infty$      free-stream static pressure, pounds/foot$^2$ (newtons/meter$^2$)

$q_\infty$      free-stream dynamic pressure, pounds/foot$^2$ (newtons/meter$^2$)

S      planform area of body, feet$^2$ (meters$^2$)

$S_{wet}$      wetted area of body (excluding base), feet$^2$ (meters$^2$)

V      volume of body, feet$^3$ (meters$^3$)

x      longitudinal coordinate

$\alpha$      angle of attack, degrees

Subscripts:

max      maximum condition

min      minimum condition

$(L/D)_{max}$      condition at maximum lift-drag ratio

o      condition at $\alpha = 0^o$

## MODELS

Drawings and photographs showing the various body cross-sectional shapes of each of the bodies tested are presented in figure 1. The changes in camber for the trapezoidal bodies E are presented in figure 2. Table I presents design ordinates for each configuration tested. Body designations as employed in the present tests are given in the following table:

| Body | Cross section | $b/l$ | K | $S_{wet}/l^2$ | Test configuration |
|------|--------------|-------|---|---------------|-------------------|
| A | Semicircular | 0.1414 | | 0.49 | { Flat top (inverted semicircle) — negative camber<br>{ Flat bottom (upright semicircle) — positive camber |
| B | Elliptic | .1414 | | .46 | { Symmetrical — no camber<br>{ Negative camber<br>{ Positive camber |
| C | Triangular | .2221 | 0 | .54 | { Flat top (inverted triangle) — negative camber<br>{ Flat bottom (upright triangle) — positive camber |
| D | Trapezoidal | .1666 | .333 | .50 | { Flat top (inverted trapezoid) — negative camber<br>{ Flat bottom (upright trapezoid) — positive camber |
| E | Trapezoidal | .1333 | .667 | .50 | { Flat top (inverted trapezoid) — negative camber<br>{ Flat bottom (upright trapezoid) — positive camber |
| $E_{mod}$ | Trapezoidal | .1333 | .667 | .50 | Flat top (upright trapezoid) — negative camber |
| F | Rectangular | .1111 | 1.000 | .52 | { Flat top — negative camber<br>{ Flat bottom — positive camber |

Each of the bodies had an equivalent fineness ratio (i.e., rates of length to equivalent circular base diameter) of 5.0. The value of $V/l^3$ was 0.016 for all bodies. The bodies had identical projected planform area, length, base area, and longitudinal distribution of cross-sectional area; the only variables were cross-sectional shape, camber, and the resultant small wetted-area changes. (See preceding table.) The longitudinal distribution of cross-sectional area for the bodies was determined from the design charts of reference 1 and represented the theoretical minimum-hypersonic-wave-drag shape under the prescribed conditions of given length and volume. The various cross sections investigated included a semicircle, an asymmetrical ellipse, a triangle, a trapezoid, and a rectangle. Each configuration was tested with both positive and negative camber. Also included was a symmetrical ellipse.

With the single exception of the symmetrical ellipse, the bodies were developed by displacing the cross sections above or below a straight horizontal line to produce positive or negative camber, respectively, as indicated in figure 1(a). An angle of attack of $0^\circ$ was assumed to exist when the straight-line surface was alined with the airstream. For the symmetrical ellipse, zero angle of attack existed when the horizontal plane of symmetry was alined with the airstream. The term "flat bottom" can be applied to positive camber and the term "flat top" can be applied to negative camber. Configuration E (fig. 2) was modified to provide negative camber to the flat-bottom upright-trapezoid shape and is designated $E_{mod}$. This modification is shown in figure 2(c).

## APPARATUS, TESTS, AND CORRECTIONS

The investigation was made in the Langley 15-inch hypersonic flow apparatus at a Mach number of 10.03. A brief description of this facility is given in reference 9. Forces and moments were measured with a sting-supported six-component water-cooled strain-gage balance. The angle-of-attack range was from approximately -5° to 21° at 0° of sideslip.

Tests were made at a stagnation temperature of approximately 1100° F (866° K) and a stagnation pressure of approximately 800 lb/sq in. (552 N/cm$^2$) which corresponds to a free-stream Reynolds number (based on body length) of $1.40 \times 10^6$. The angle of attack has been corrected for sting and balance deflections under load. Axial-force data have not been corrected for the effects of base pressure; however, base-pressure measurements were made and are presented in figure 3 as base axial-force coefficients.

## DISCUSSION

Basic longitudinal aerodynamic characteristics associated with each of the six configurations tested are presented in figure 4. Summary plots of various longitudinal aerodynamic parameters noted for each of the bodies are given in figures 5 and 6 to illustrate more clearly the effects of changes in cross-sectional shape and in camber.

### Effects of Cross Section

The planform area, base area, longitudinal area distribution, and span are all constant for each of the configurations tested, the only variables being cross-sectional shape, camber, and small changes in wetted area. There are little or no effects of changing cross-sectional shape on the minimum-drag characteristics of any of the configurations with either positive or negative camber. (See figs. 5 and 6.) It is interesting to note that the body does not have to be symmetrical for retention of the low $C_{D,min}$ characteristics, as long as the body is relatively slender in the longitudinal sense (i.e., local body slope is much less than 1.0), as noted in the slender-body approximation of reference 10. However, the theory allows no change in cross-sectional shape along the length of the body. The normalized longitudinal area distributions for minimizing hypersonic zero-lift pressure drag under prescribed conditions of given length and volume shown in reference 1 for circular or elliptic bodies, therefore, are not only insensitive to changes in fineness ratio from 3.09 to 30.00, as indicated in the appendix of reference 1, but are also apparently insensitive to cross-sectional shape changes.

The effects of changing cross section on the $(L/D)_{max}$ characteristics of the various bodies are summarized in figures 5 and 6. Increases in $(L/D)_{max}$ and

$C_{L,(L/D)_{max}}$ (fig. 5) occur for the flat-bottom (i.e., positive camber) bodies. This improvement becomes more pronounced as the body height is increased. Since the planform area and the cross-sectional area are fixed, increasing the body height results in an inward movement of the lateral or side surfaces, so that increasing amounts of shadowing of these side surfaces occur. This result suggests that the lift and cross-flow drag approach values that would be obtained for a simple flat plate. Since the cross-flow drag component, which contributes directly to second-order lift effects even at high supersonic speeds (ref. 11), would be maximum for a flat plate, the triangular body, which more nearly approaches this condition, shows both the higher $C_{L,(L/D)_{max}}$ and corresponding $(L/D)_{max}$ (fig. 5).

Since one purpose of the investigation was to examine methods of increasing both the $(L/D)_{max}$ and $C_{L,(L/D)_{max}}$ characteristics of minimum wave-drag bodies over those obtained on elliptic bodies, a comparison of these characteristics is shown in figure 6 for the various configurations tested. The $(L/D)_{max}$ and $C_{L,(L/D)_{max}}$ values of each body with positive camber have been normalized with respect to the values obtained for the elliptic body with positive camber. Similarly, the characteristics of the bodies with negative camber have been normalized with respect to the ellipse with negative camber. Improvement in both $(L/D)_{max}$ and $C_{L,(L/D)_{max}}$ over the values noted for the elliptic bodies was noted for each of the bodies whose major cross-sectional width was at the bottom. This improvement was independent of camber and is best illustrated by examination of the results of camber reversal on upright trapezoidal configuration E.

### Effects of Camber

The major portion of the bodies having positive camber also had the maximum cross-sectional width at the bottom; that is, their cross sections were upright triangles, trapezoids, or semicircles. As noted in figures 5 and 6, these bodies always showed higher values of untrimmed $(L/D)_{max}$ than either the elliptic bodies or the bodies having negative camber. The resultant moment characteristics, however, indicate large out-of-trim $C_{m,(L/D)_{max}}$ (fig. 4) for the bodies having positive camber, whereas favorable $C_m$ characteristics (i.e., positive $C_{m,o}$) were noted for the bodies having negative camber. For a particular configuration (upright trapezoidal cross section E), camber was reversed from positive to negative in an effort to combine the high $(L/D)_{max}$ and $C_{L,(L/D)_{max}}$ characteristics with favorable $C_m$.

The effect of camber is illustrated in figure 5. For the modified trapezoidal configuration, designated $E_{mod}$, the $(L/D)_{max}$ and $C_{L,(L/D)_{max}}$ characteristics are comparable to those noted for the upright cross section E with positive camber. In addition, favorable (positive) $C_m$ characteristics were obtained. It is also interesting to note that the angle of attack for $(L/D)_{max}$ for the $E_{mod}$ configuration was greatly reduced as compared with the value obtained for body E with positive camber.

## SUMMARY OF RESULTS

An investigation has been made at hypersonic speeds of a series of bodies having variations in cross-sectional shape and camber. The longitudinal distribution of cross-sectional area for each body conformed to the theoretical shape required to minimize the zero-lift hypersonic pressure drag of circular or elliptic bodies under the geometric constraints of given length and volume. Each body tested had constant planform area, base area, and span; the only variables were cross-sectional shape, camber, and the resultant small wetted-area changes. Cross sections tested included semicircular, elliptic, triangular, trapezoidal, and rectangular shapes. Results of the investigation may be summarized in the following observations:

1. Changing cross-sectional shape had essentially no effect on the minimum-drag characteristics of any configuration tested. Furthermore, camber had little or no effect on these characteristics.

2. For all cross sections investigated, the highest values of untrimmed maximum lift-drag ratio and lift at maximum untrimmed lift-drag ratio were obtained for the flat-bottom (positive camber) bodies having upright semicircular, trapezoidal, or triangular cross sections; that is, cross sections having maximum width at the bottom. Large out-of-trim (negative) pitching moments at maximum lift-drag ratio were noted, however, for these bodies with positive camber. The bodies with negative camber produced favorable (positive) pitching moments and a considerable reduction in the angle of attack for maximum lift-drag ratio as compared with that obtained for the bodies with positive camber.

3. Reversing the camber from positive to negative for an upright trapezoidal configuration (that is, a configuration having its major horizontal cross-sectional area at the bottom) resulted in essentially the same values of maximum lift-drag ratio and lift at maximum lift-drag ratio as had been noted before the reversal of camber. This reversal

8

to negative camber also provided favorable pitching-moment characteristics and resultantly large reductions in the angle of attack for maximum lift-drag ratio.
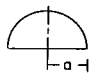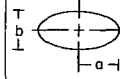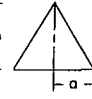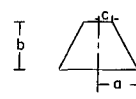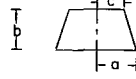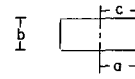
Langley Research Center,
National Aeronautics and Space Administration,
Langley Station, Hampton, Va., February 1, 1967,
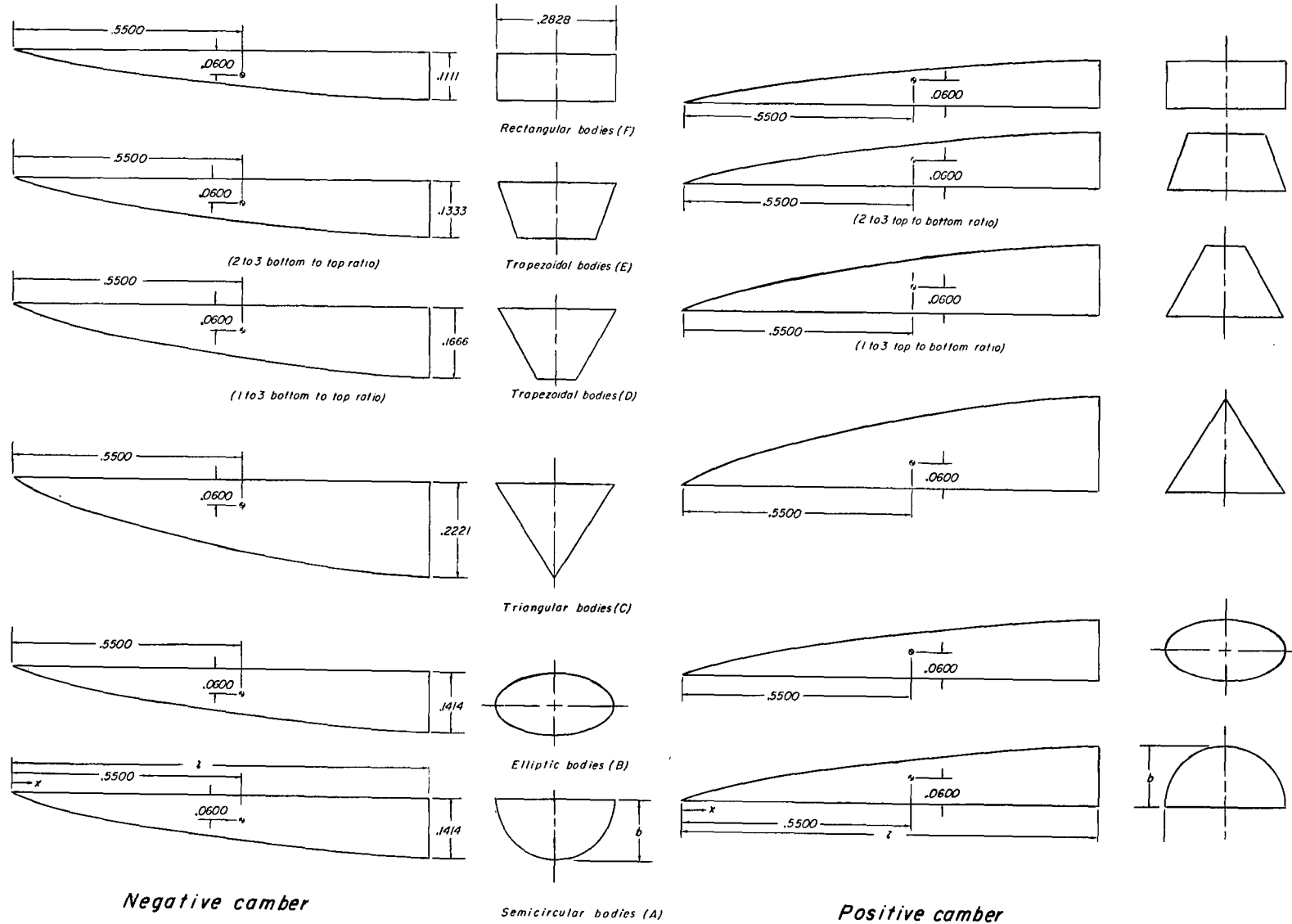126-13-03-20-23.

# REFERENCES

1. Spencer, Bernard, Jr.; and Fox, Charles H., Jr.: Hypersonic Aerodynamic Performance of Minimum-Wave-Drag Bodies. NASA TR R-250, 1966.

2. Becker, John V.: Studies of High Lift/Drag Ratio Hypersonic Configurations. Proceedings of the 4th Congress of the International Council of the Aeronautical Sciences, Robert R. Dexter, ed., Spartan Books, Inc., 1965, pp. 877-910.

3. Fetterman, David E.; Henderson, Arthur, Jr.; Bertram, Mitchel H.; and Johnson, Patrick J.: Studies Relating to the Attainment of High Lift-Drag Ratios at Hypersonic Speeds. NASA TN D-2956, 1965.

4. Miele, Angelo; and Huang, Ho-Yi: Power-Law Bodies of Maximum Lift-to-Drag Ratio in Hypersonic Flow. Aero-Astronaut. Rept. No. 20, Grant No. NGR-44-006-034, Rice Univ., 1966.

5. Lusty, Arthur H., Jr.; and Miele, Angelo: Bodies of Maximum Lift-to-Drag Ratio in Hypersonic Flow. Aero-Astronaut. Rept. No. 22, Grant No. NGR-44-006-034, Rice Univ., 1966.

6. Eggers, A. J., Jr.; Resnikoff, Meyer M.; and Dennis, David H.: Bodies of Revolution Having Minimum Drag at High Supersonic Airspeeds. NACA Rept. 1306, 1957. (Supersedes NACA TN 3666.)

7. Suddath, Jerrold H.; and Oehman, Waldo I.: Minimum Drag Bodies With Cross-Sectional Ellipticity. NASA TN D-2432, 1964.

8. Miele, Angelo: Similarity Laws for Optimum Hypersonic Bodies. Astronaut. Acta, vol. II, no. 3, 1965, pp. 202-206.

9. Putnam, Lawrence E.; and Brooks, Cuyler W., Jr.: Static Longitudinal Aerodynamic Characteristics at a Mach Number of 10.03 of Low-Aspect-Ratio Wing-Body Configurations Suitable for Reentry. NASA TM X-733, 1962.

10. Miele, Angelo: Slender Shapes of Minimum Drag in Newtonian Flow. Z. Flugwissenschaften, Jahrg. 11, Heft 5, May 1963, pp. 203-210.

11. Jorgensen, Leland H.: Elliptic Cones Alone and With Wings at Supersonic Speeds. NACA Rept. 1376, 1958. (Supersedes NACA TN 4045.)

## TABLE I.- BODY ORDINATES

$$[S = 0.1274 \text{ ft}^2 \ (0.0118 \text{ m}^2); \ \ell = 10.00 \text{ in.} \ (25.40 \text{ cm}); \ 2a = 2.828 \text{ in.} \ (7.1831 \text{ cm})]$$

| | Body A | | Body B | Body C | Body D | | Body E | | Body F | |
|---|---|---|---|---|---|---|---|---|---|---|
| $x/\ell$ | $a/\ell$ | $b/\ell$ | $b/\ell$ | $b/\ell$ | $b/\ell$ | $c/\ell$ | $b/\ell$ | $c/\ell$ | $b/\ell$ | $c/\ell$ |
| 0 | 0 | 0 | 0 | 0 | 0 | 0 | 0 | 0 | 0 | 0 |
| .006 | .0042 | .0042 | .0042 | .0067 | .0050 | .0014 | .0040 | .0028 | .0033 | .0042 |
| .008 | .0047 | .0047 | .0047 | .0074 | .0055 | .0016 | .0044 | .0031 | .0037 | .0047 |
| .010 | .0063 | .0063 | .0063 | .0099 | .0074 | .0021 | .0060 | .0042 | .0050 | .0063 |
| .015 | .0077 | .0077 | .0077 | .0122 | .0091 | .0026 | .0073 | .0052 | .0061 | .0077 |
| .020 | .0095 | .0095 | .0095 | .0149 | .0112 | .0032 | .0089 | .0063 | .0074 | .0095 |
| .030 | .0129 | .0129 | .0129 | .0202 | .0152 | .0043 | .0121 | .0086 | .0101 | .0129 |
| .040 | .0161 | .0161 | .0161 | .0253 | .0190 | .0054 | .0152 | .0108 | .0127 | .0161 |
| .050 | .0190 | .0190 | .0190 | .0299 | .0224 | .0063 | .0179 | .0127 | .0149 | .0190 |
| .060 | .0219 | .0219 | .0219 | .0343 | .0258 | .0073 | .0206 | .0146 | .0172 | .0219 |
| .070 | .0245 | .0245 | .0245 | .0385 | .0289 | .0082 | .0231 | .0163 | .0192 | .0245 |
| .080 | .0270 | .0270 | .0270 | .0424 | .0318 | .0090 | .0255 | .0180 | .0212 | .0270 |
| .090 | .0297 | .0297 | .0297 | .0466 | .0349 | .0099 | .0280 | .0198 | .0233 | .0297 |
| .100 | .0320 | .0320 | .0320 | .0503 | .0377 | .0107 | .0302 | .0213 | .0251 | .0320 |
| .120 | .0370 | .0370 | .0370 | .0581 | .0436 | .0123 | .0349 | .0247 | .0291 | .0370 |
| .140 | .0411 | .0411 | .0411 | .0646 | .0484 | .0137 | .0387 | .0274 | .0323 | .0411 |
| .160 | .0453 | .0453 | .0453 | .0711 | .0533 | .0151 | .0427 | .0302 | .0356 | .0453 |
| .200 | .0534 | .0534 | .0534 | .0839 | .0629 | .0178 | .0503 | .0356 | .0419 | .0534 |
| .240 | .0607 | .0607 | .0607 | .0953 | .0715 | .0202 | .0572 | .0404 | .0476 | .0607 |
| .280 | .0677 | .0677 | .0677 | .1063 | .0797 | .0226 | .0638 | .0451 | .0532 | .0677 |
| .320 | .0741 | .0741 | .0741 | .1164 | .0873 | .0247 | .0698 | .0494 | .0582 | .0741 |
| .360 | .0803 | .0803 | .0803 | .1262 | .0946 | .0268 | .0757 | .0535 | .0631 | .0803 |
| .400 | .0861 | .0861 | .0861 | .1353 | .1015 | .0287 | .0812 | .0574 | .0677 | .0861 |
| .440 | .0920 | .0920 | .0920 | .1445 | .1084 | .0307 | .0867 | .0613 | .0722 | .0920 |
| .480 | .0975 | .0975 | .0975 | .1531 | .1148 | .0325 | .0919 | .0650 | .0766 | .0975 |
| .520 | .1029 | .1029 | .1029 | .1616 | .1212 | .0343 | .0969 | .0686 | .0808 | .1029 |
| .580 | .1100 | .1100 | .1100 | .1728 | .1296 | .0367 | .1037 | .0733 | .0864 | .1100 |
| .660 | .1187 | .1187 | .1187 | .1864 | .1398 | .0396 | .1118 | .0791 | .0932 | .1187 |
| .720 | .1245 | .1245 | .1245 | .1956 | .1467 | .0415 | .1173 | .0830 | .0978 | .1245 |
| .780 | .1296 | .1296 | .1296 | .2036 | .1527 | .0432 | .1222 | .0864 | .1018 | .1296 |
| .840 | .1342 | .1342 | .1342 | .2107 | .1581 | .0447 | .1265 | .0894 | .1054 | .1342 |
| .900 | .1379 | .1379 | .1379 | .2166 | .1625 | .0460 | .1300 | .0919 | .1083 | .1379 |
| .920 | .1390 | .1390 | .1390 | .2181 | .1636 | .0463 | .1309 | .0926 | .1091 | .1390 |
| .940 | .1398 | .1398 | .1398 | .2195 | .1646 | .0466 | .1317 | .0932 | .1098 | .1393 |
| .960 | .1405 | .1405 | .1405 | .2207 | .1655 | .0468 | .1324 | .0937 | .1104 | .1405 |
| .970 | .1408 | .1408 | .1408 | .2212 | .1659 | .0469 | .1328 | .0939 | .1106 | .1408 |
| .980 | .1411 | .1411 | .1411 | .2216 | .1662 | .0470 | .1330 | .0941 | .1108 | .1411 |
| .990 | .1413 | .1413 | .1413 | .2219 | .1664 | .0471 | .1332 | .0942 | .1110 | .1413 |
| 1.000 | .1414 | .1414 | .1414 | .2221 | .1666 | .0471 | .1333 | .0943 | .1111 | .1414 |

.5500
.0600
.1111

.2828
Rectangular bodies (F)

.5500
.0600
.1333

(2 to 3 bottom to top ratio)
Trapezoidal bodies (E)

.5500
.0600
.1666

(1 to 3 bottom to top ratio)
Trapezoidal bodies (D)

.5500
.0600
.2221

Triangular bodies (C)

.5500
.0600
.1414

Elliptic bodies (B)

ℓ
.5500
x
.0600
.1414

Semicircular bodies (A)
b

Negative camber

.5500
.0600

(2 to 3 top to bottom ratio)

.5500
.0600

(1 to 3 top to bottom ratio)

.5500
.0600

.5500
.0600

.5500
x
.0600
b
ℓ

Positive camber

(a) Drawings. All dimensions are normalized with respect to maximum body length and all configurations are shown at $\alpha = 0^0$ condition.

Figure 1.- Various models tested.
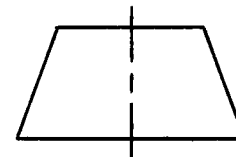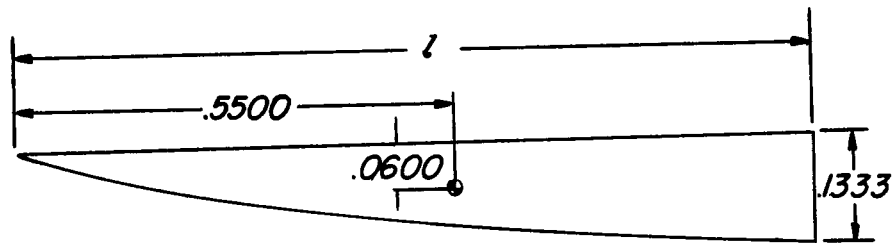
Modified trapezoidal body (E)
Negative camber
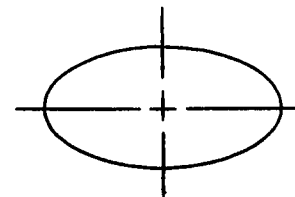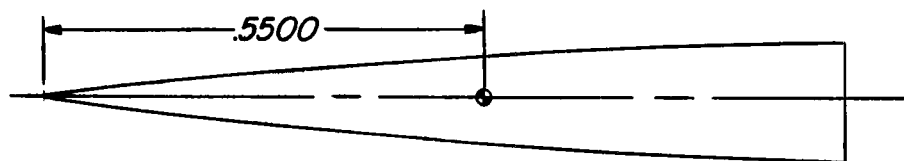
Symmetrical elliptic body (B)

(a) Concluded.

Figure 1.- Continued.

A
Semi-
circular    B
Elliptic    C
Triangular   D
Trapezoidal   E
Trapezoidal   F
Rectangular    L-66-4124

A
Semi-
circular    B
Elliptic    C
Triangular   D
Trapezoidal   E
Trapezoidal   F
Rectangular
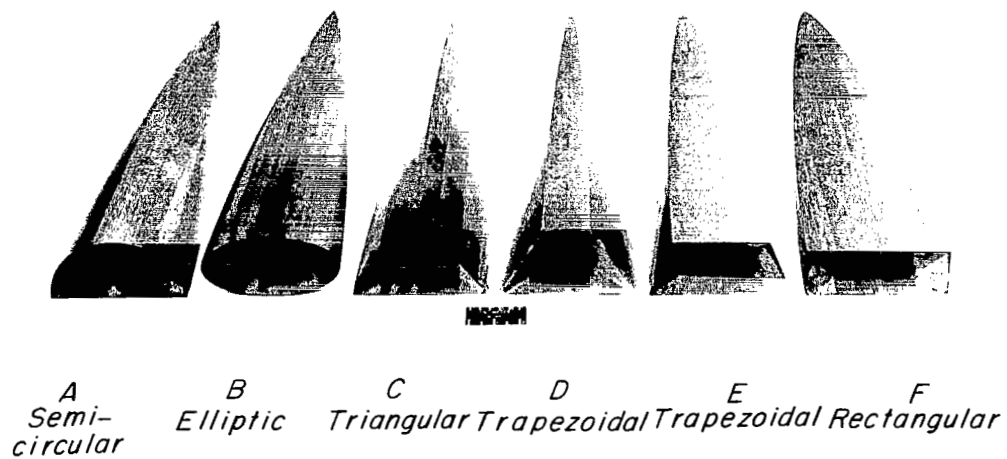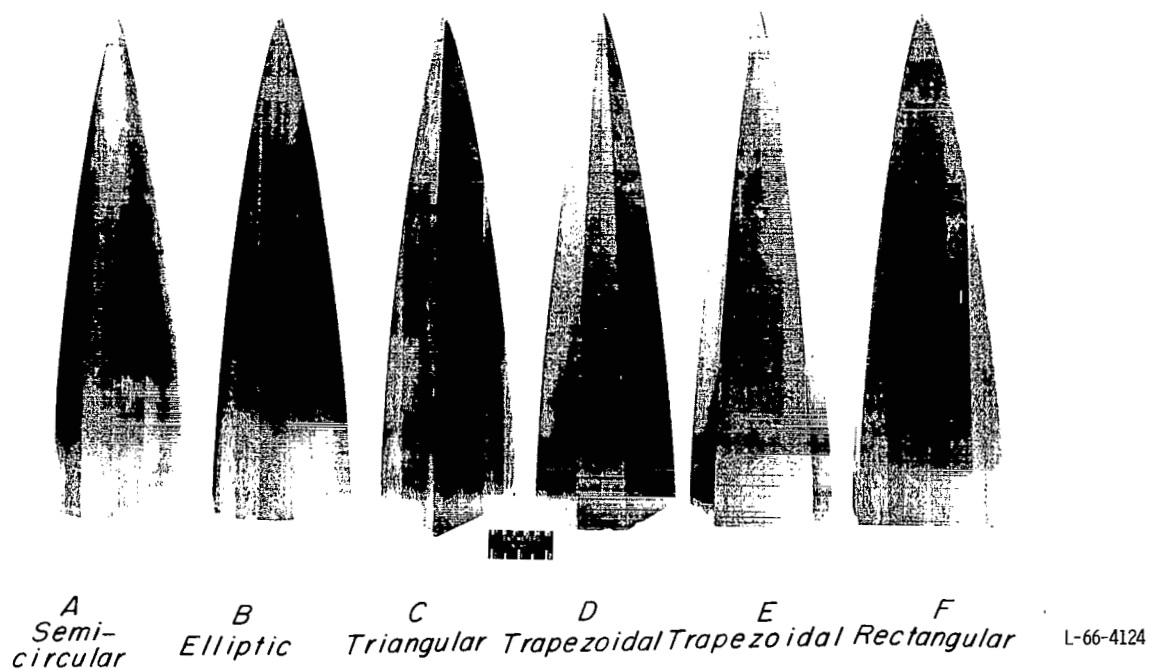
(b) Photographs of models representative of configurations tested.     L-66-4119

Figure 1.- Concluded.

14

(a) Flat-bottom upright-trapezoid E. ($\alpha = 0^0$ condition; maximum width of cross section at bottom, which is parallel to flow; positive camber.)
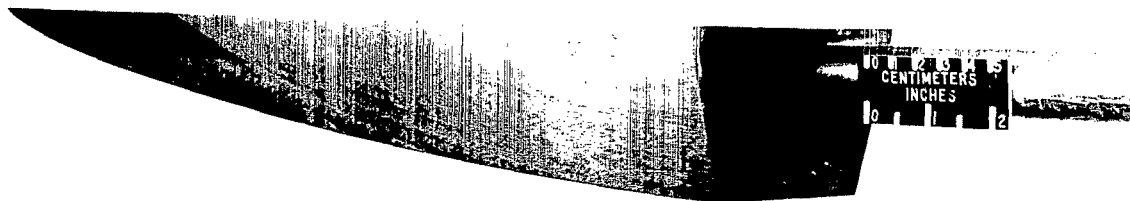


(b) Flat-top inverted-trapezoid E. ($\alpha = 0^0$ condition; maximum width of cross section at top, which is parallel to flow; negative camber.)



(c) Modified flat-top upright-trapezoid $E_{mod}$. ($\alpha = 0^0$ condition; maximum width of cross section at bottom; flow parallel to top; negative camber.)

Figure 2.- Photographs showing changes in camber for trapezoidal bodies E.            L-67-1050
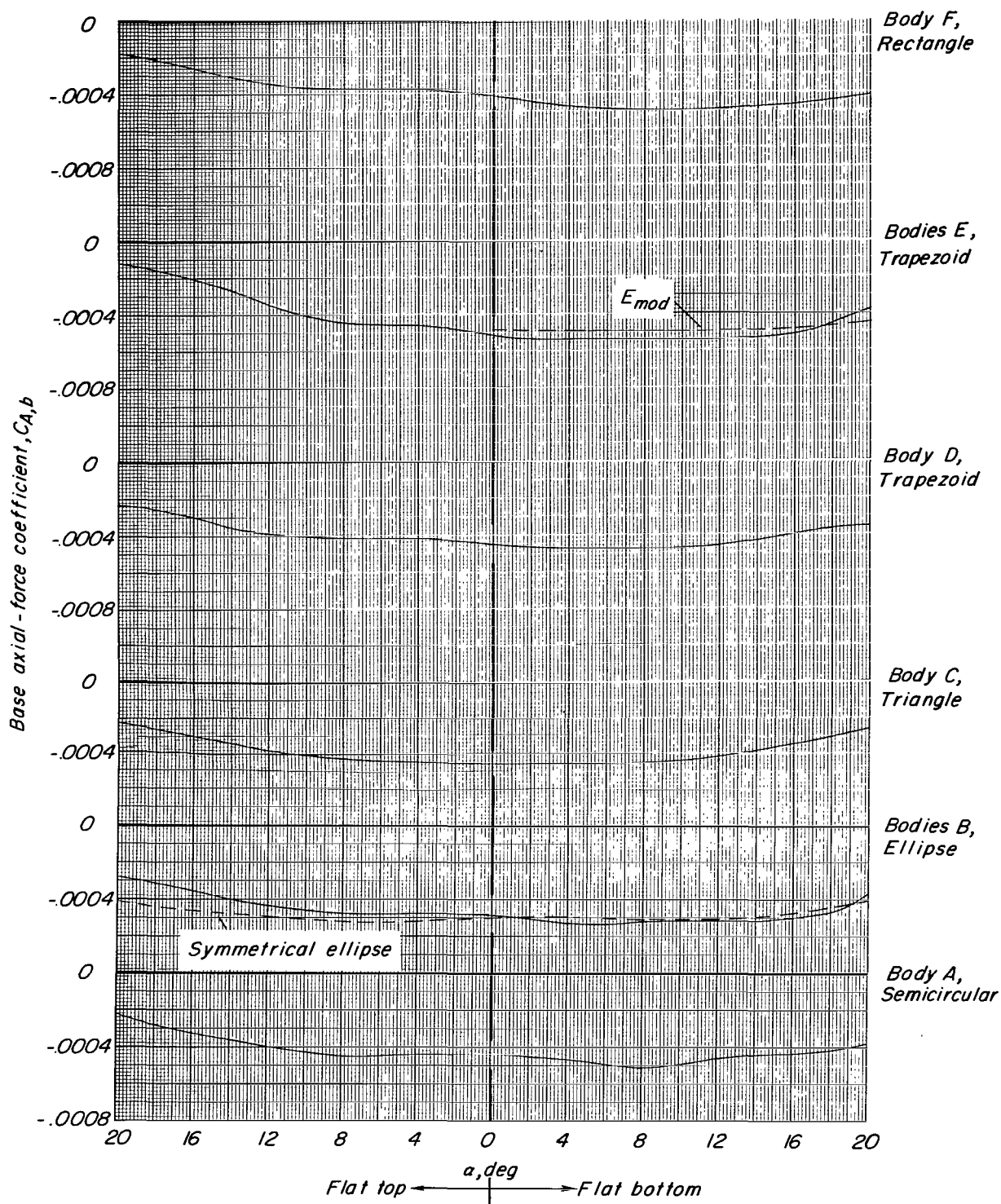
Figure 3.- Base axial-force characteristics of the various configurations tested.
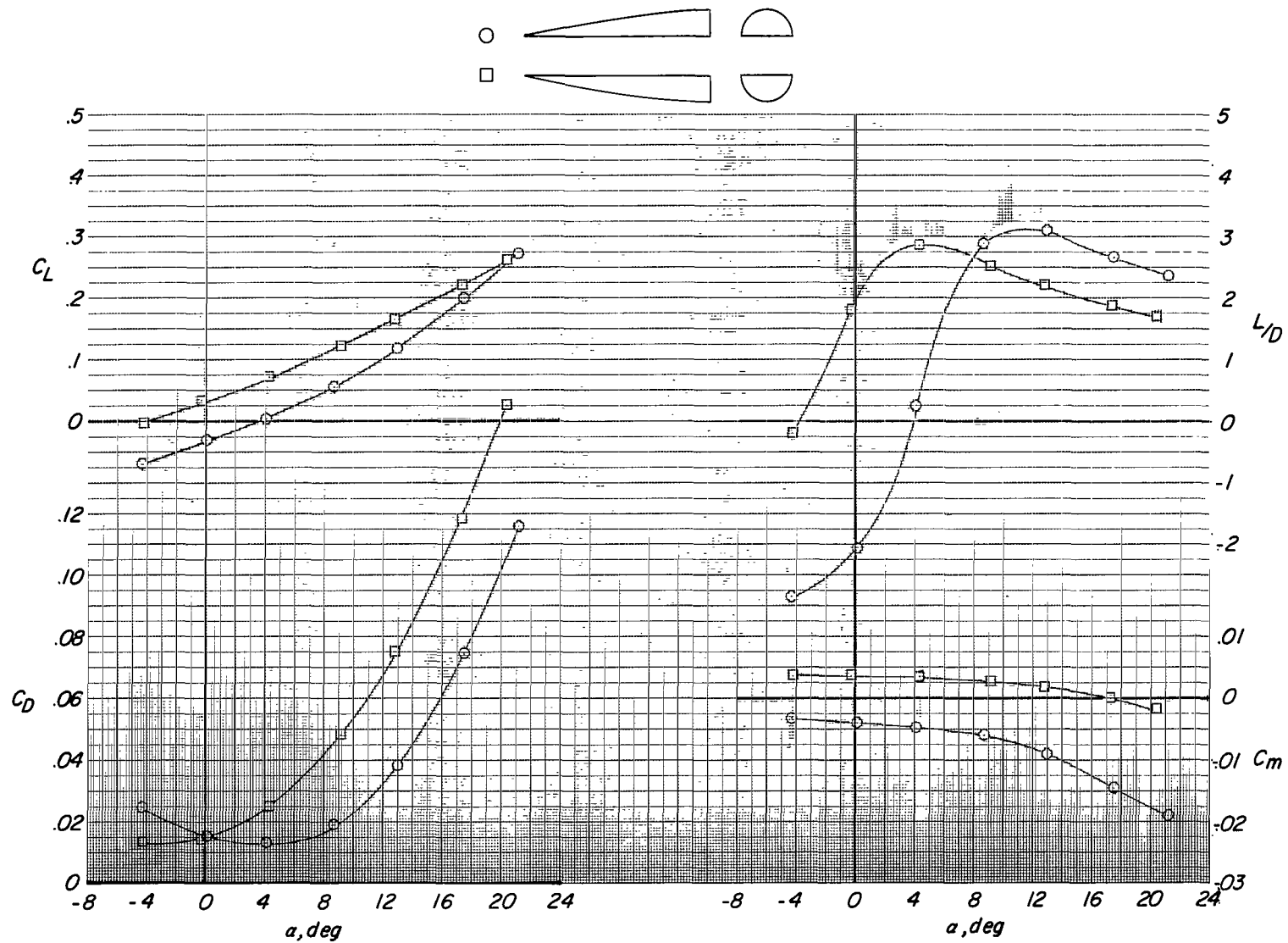
(a) Bodies A (semicircular cross sections).

Figure 4.- Longitudinal aerodynamic characteristics of the various configurations tested. $M_\infty = 10.03$.
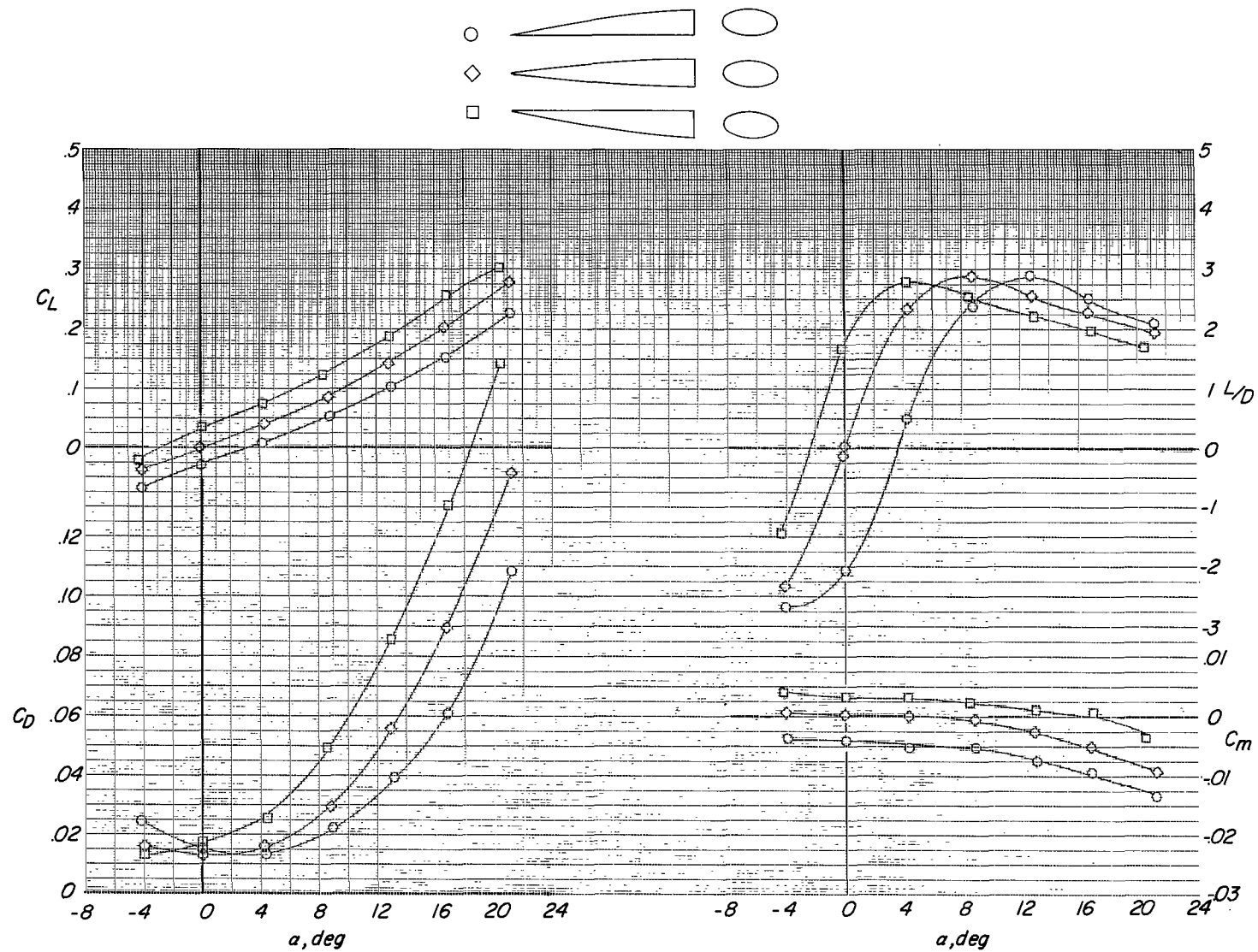
(b) Bodies B (elliptic cross sections).

Figure 4.- Continued.
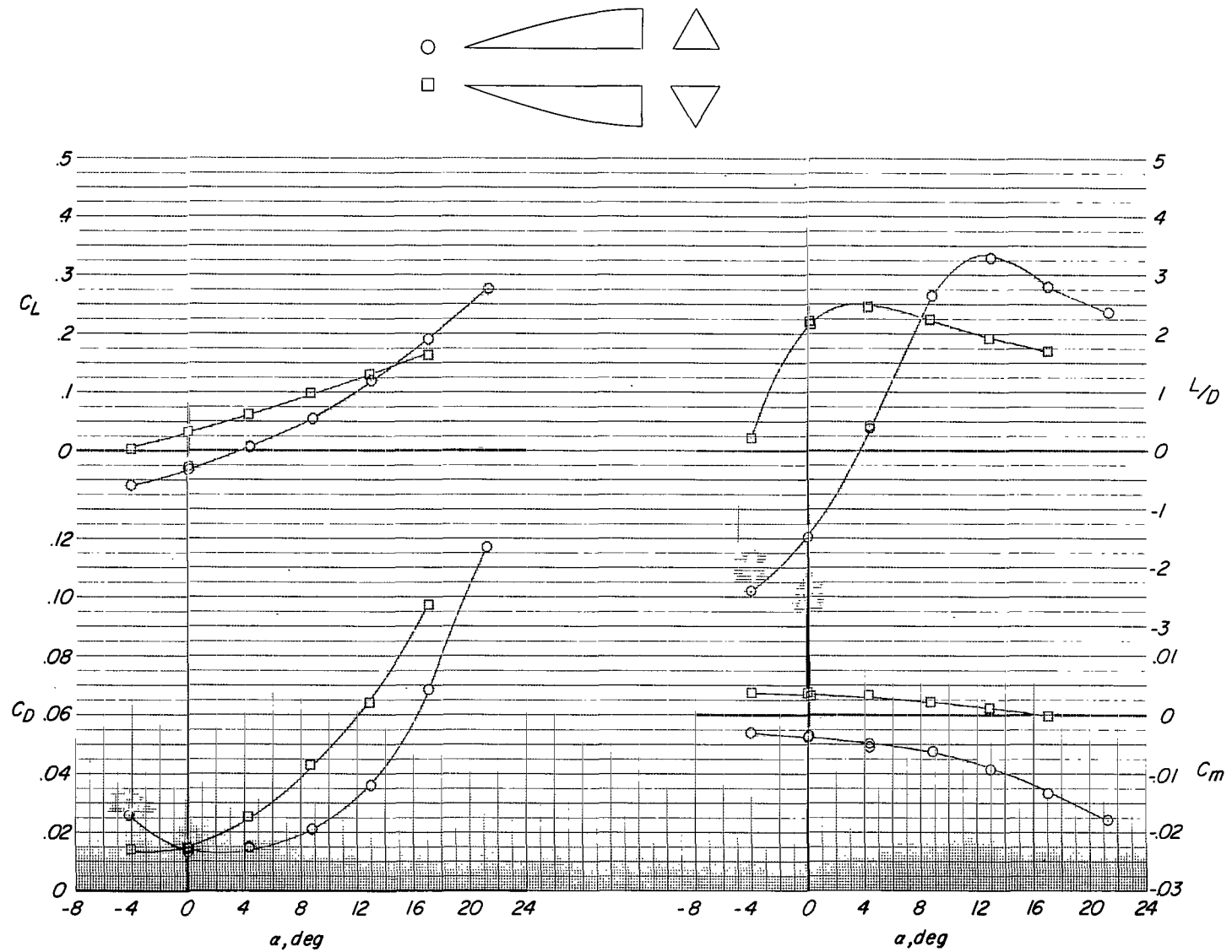
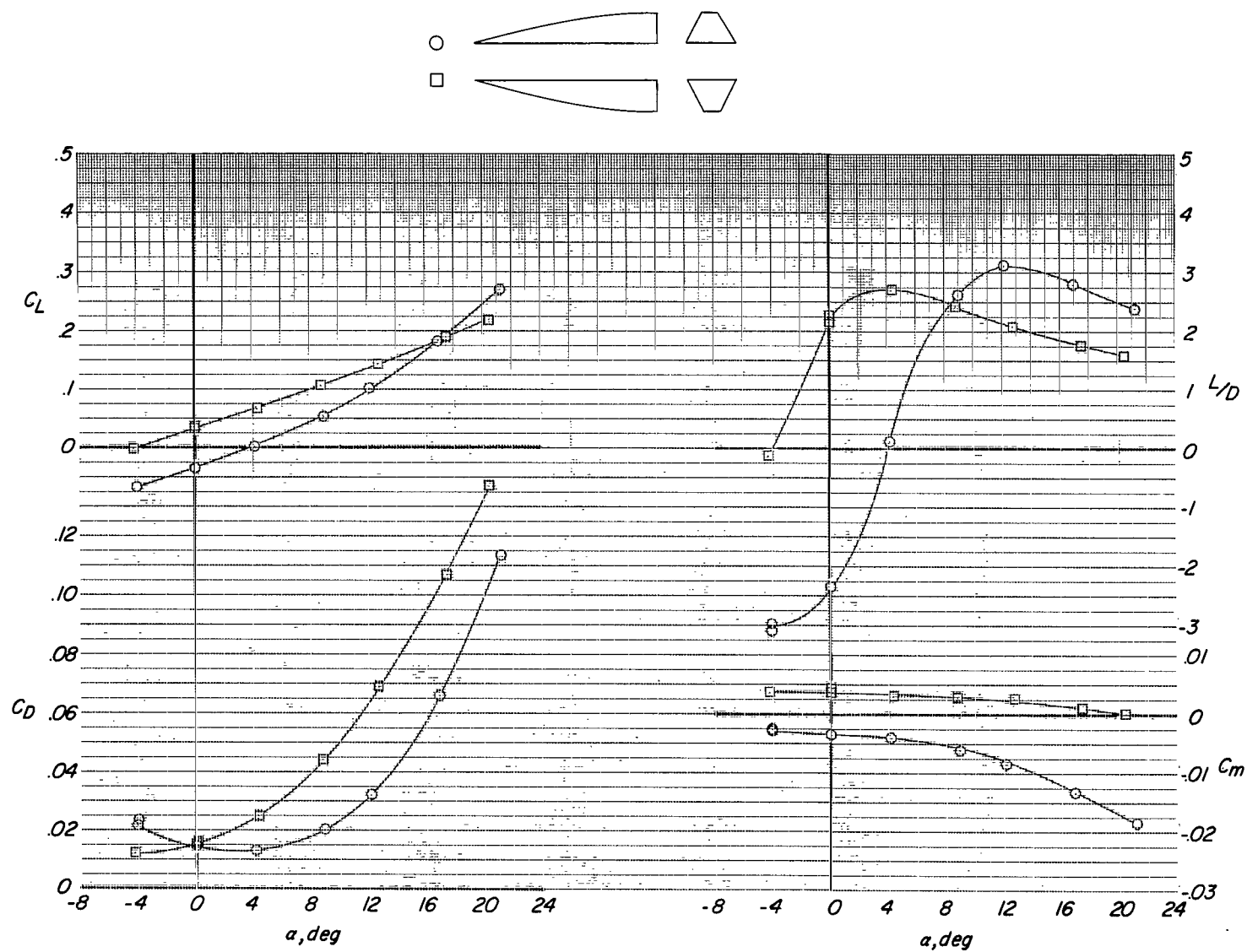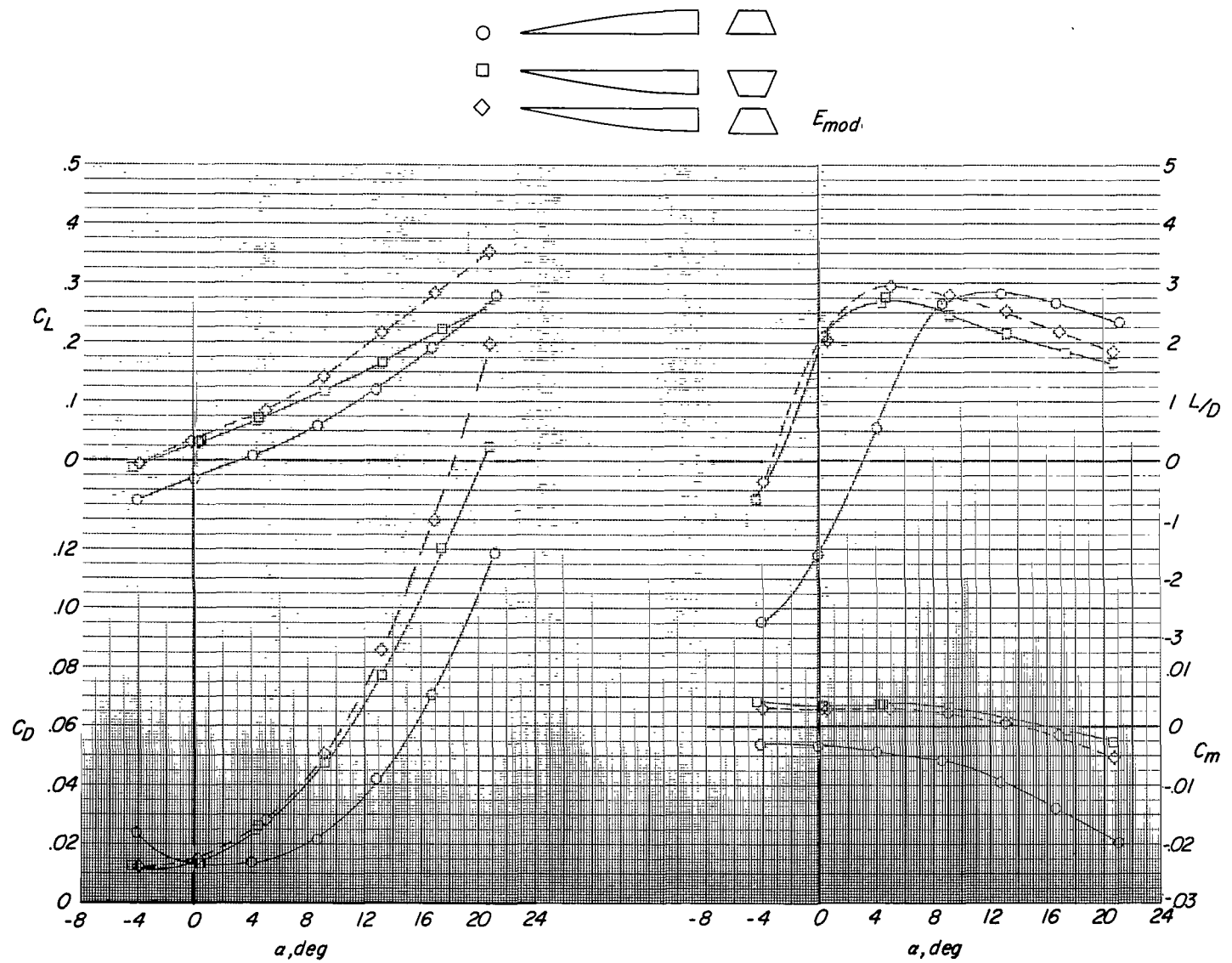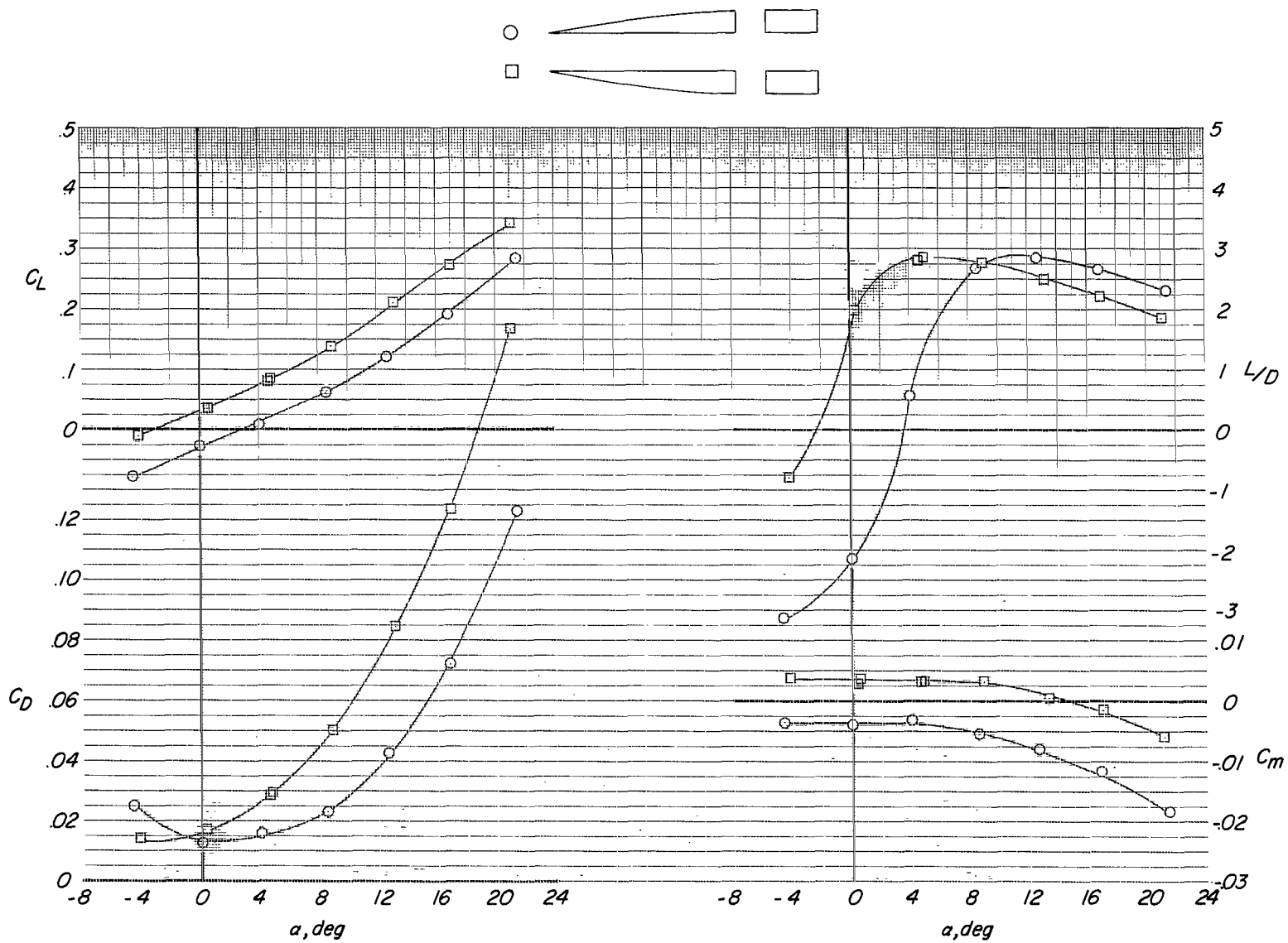(c) Bodies C (triangular cross sections).

Figure 4.- Continued.

(d) Bodies D (trapezoidal cross sections). K = 0.333.

Figure 4.- Continued.

(e) Bodies E (trapezoidal cross sections).  K = 0.667.

Figure 4.- Continued.

(f) Bodies F (rectangular cross sections).
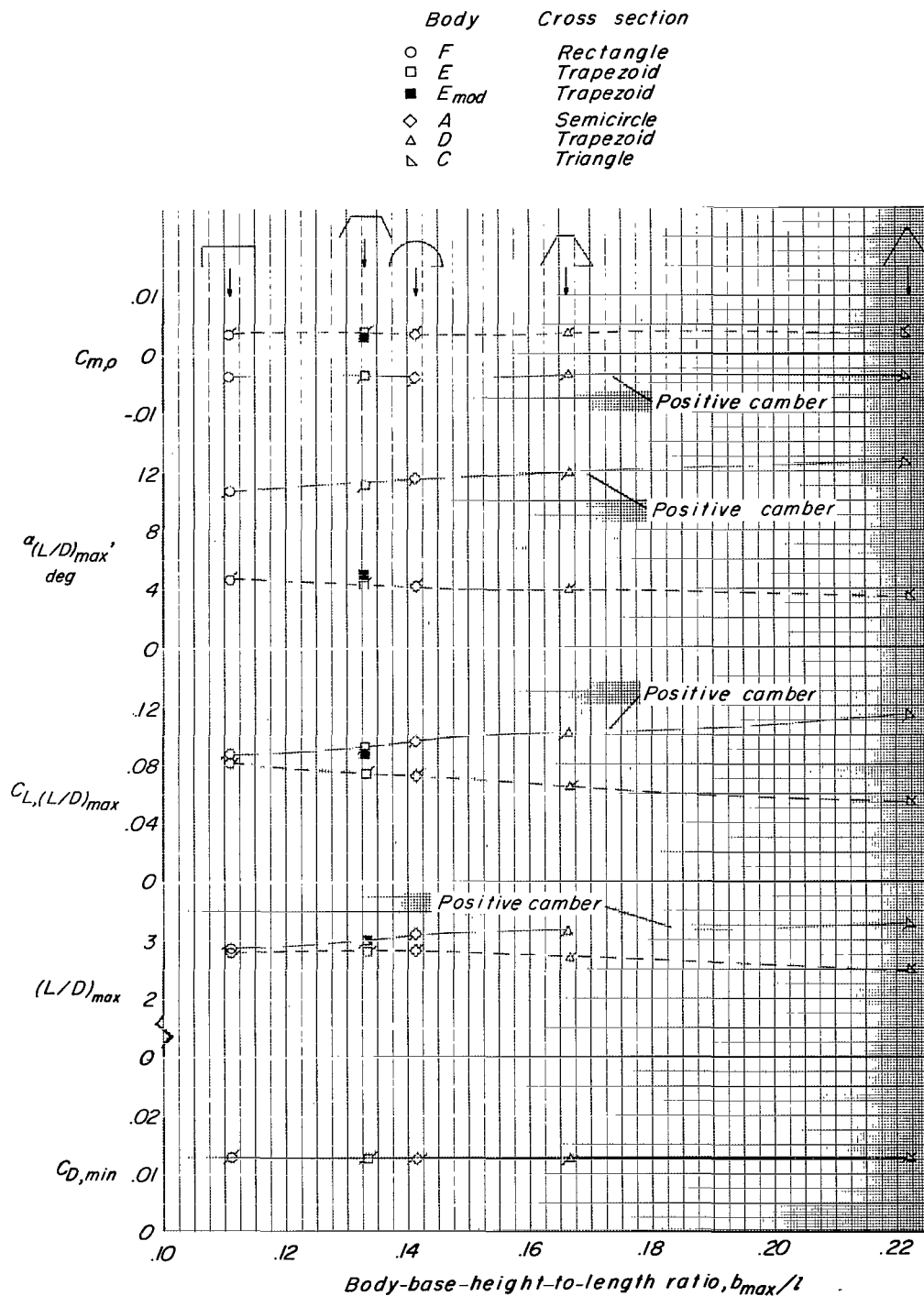
Figure 4.- Concluded.

Figure 5.- Summary of pertinent longitudinal aerodynamic parameters associated with each configuration tested, excluding elliptic bodies. Flags on lower part of symbols indicate positive camber, and flags on upper part of symbols indicate negative camber.

Body | Cross section
:--- | :---
○ F | Rectangle
□ E | Trapezoid
■ $E_{mod}$ | Trapezoid
◇ A | Semicircle
△ D | Trapezoid
◺ C | Triangle

$$\frac{C_{L,(L/D)_{max}}}{C_{L,(L/D)_{max(ellipse)}}}$$

1.3 1.2 1.1 1.0 .9 .8 .7

Positive camber

$$\frac{(L/D)_{max}}{(L/D)_{max(ellipse)}}$$

1.2 1.1 1.0 .9 .8

Positive camber

$$\frac{C_{D,min}}{C_{D,min(ellipse)}}$$

1.1 1.0 .9

.10 .12 .14 .16 .18 .20 .22

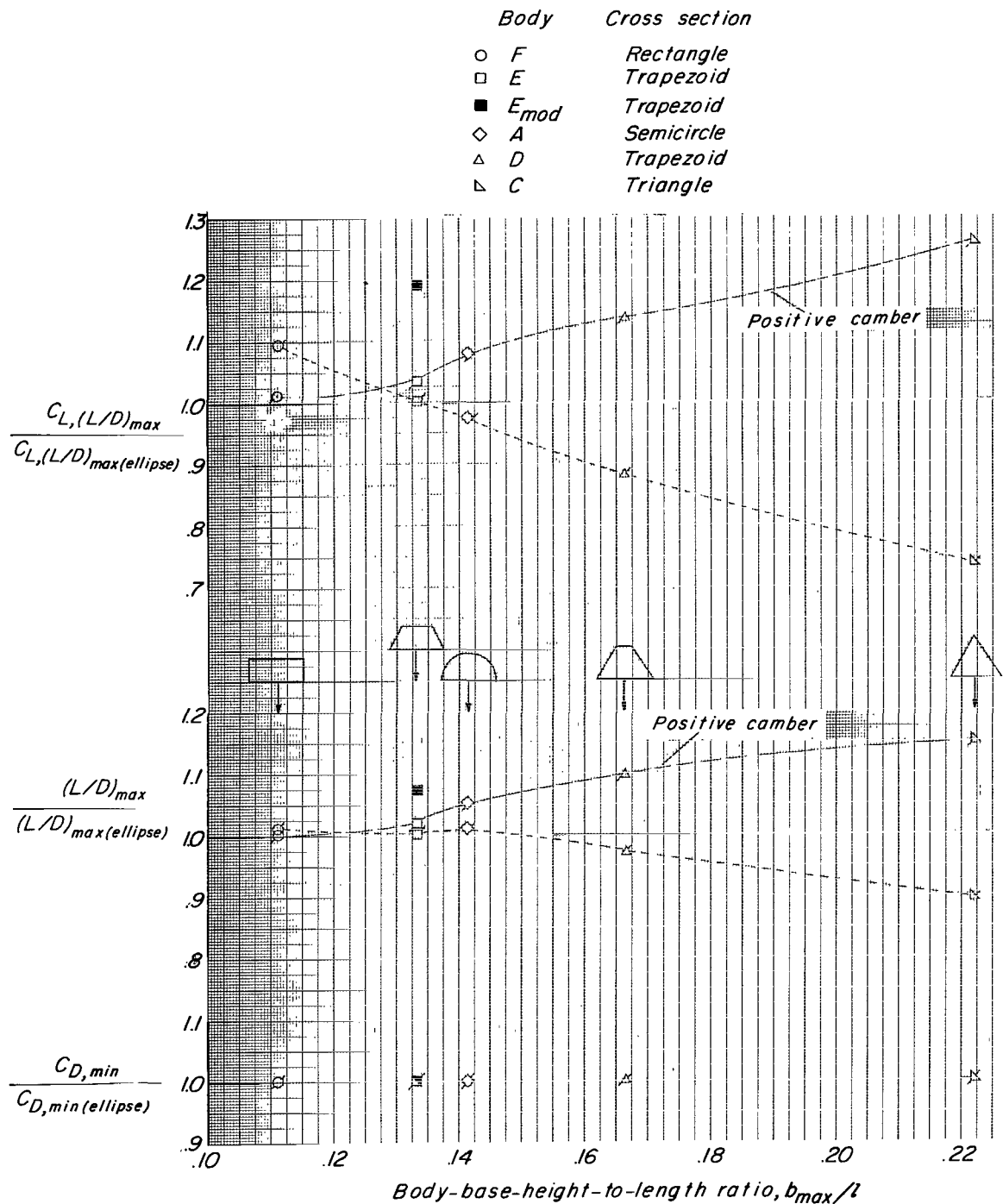Body-base-height-to-length ratio, $b_{max}/l$

Figure 6.- Comparison of various longitudinal aerodynamic parameters associated with the various configurations tested as weighted by values obtained on basic ellipses. Flags on lower part of symbols indicate positive camber, and flags on upper part of symbols indicate negative camber.

# NASA SCIENTIFIC AND TECHNICAL PUBLICATIONS

**TECHNICAL REPORTS:** Scientific and technical information considered important, complete, and a lasting contribution to existing knowledge.

**TECHNICAL NOTES:** Information less broad in scope but nevertheless of importance as a contribution to existing knowledge.

**TECHNICAL MEMORANDUMS:** Information receiving limited distribution because of preliminary data, security classification, or other reasons.

**CONTRACTOR REPORTS:** Scientific and technical information generated under a NASA contract or grant and considered an important contribution to existing knowledge.

**TECHNICAL TRANSLATIONS:** Information published in a foreign language considered to merit NASA distribution in English.

**SPECIAL PUBLICATIONS:** Information derived from or of value to NASA activities. Publications include conference proceedings, monographs, data compilations, handbooks, sourcebooks, and special bibliographies.

**TECHNOLOGY UTILIZATION PUBLICATIONS:** Information on technology used by NASA that may be of particular interest in commercial and other non-aerospace applications. Publications include Tech Briefs, Technology Utilization Reports and Notes, and Technology Surveys.

*Details on the availability of these publications may be obtained from:*

SCIENTIFIC AND TECHNICAL INFORMATION DIVISION

## NATIONAL AERONAUTICS AND SPACE ADMINISTRATION

Washington, D.C. 20546